

Determination of Boundary Scattering, Intermagnon Scattering, and the Haldane Gap in Heisenberg Chains

Hiroshi UEDA* and Koichi KUSAKABE†

Graduate School of Engineering Science, Osaka University, Toyonaka, Osaka 560-8531, Japan

(Dated: December 6, 2018)

Low-lying magnon dispersion in a $S = 1$ Heisenberg antiferromagnetic (AF) chain is analyzed using the non-Abelian DMRG method. The scattering length a_b of the boundary coupling and the inter-magnon scattering length a are determined. The scattering length a_b is found to exhibit a characteristic diverging behavior at the crossover point. In contrast, the Haldane gap Δ , the magnon velocity v , and a remain constant at the crossover. Our method allowed estimation of the gap of the $S = 2$ AF chain to be $\Delta = 0.0891623(9)$ using a chain length longer than the correlation length ξ .

PACS numbers: 75.10.Jm, 75.40.Mg

I. INTRODUCTION

To form a better understanding of interacting many-body systems, it is very important to determine an effective field theory and to clarify the low-energy physics involved. In the physics of low-dimensional quantum systems, considerable attention has been paid to the one-dimensional antiferromagnetic (AF) integer-spin Heisenberg model following the discovery of the Haldane gap.^{34,35} Precise determination of the gap has been reported by several authors.^{36–40} Its massive elementary excitation, *i.e.*, the magnon, has a relativistic dispersion relation, which is often described by a non-linear sigma model (NLSM).^{34,35,41,42}

In particular, the $S = 1$ AF Heisenberg chain has been widely studied both theoretically and experimentally. When open boundary conditions (OBC) are applied to a $S = 1$ AF chain, owing to the unique effective $S = 1/2$ spins at the ends, quasi-degeneracy appears between the singlet ground state and a low-lying triplet state.⁴³ Various attempts at boundary tuning,³⁶ as exemplified by attachment of real $S = 1/2$ spins to maintain the high accuracy of the density matrix renormalization group (DMRG) method,^{44,45} have shown that deformation of the boundary conditions can selectively modify the magnon wavefunction while maintaining the uniformity of the ground state.⁴⁶

To form a better understanding of the physics involved in a finite chain under OBC, we can use the NLSM to describe the low-lying energy dispersion. Lou *et al.* have proposed usage of a form, $\sqrt{\Delta^2 + v^2 \sin^2 k_{\text{eff}}}$, for low-lying magnon dispersions, where k_{eff} is the effective wavenumber.⁴⁷ Here, Δ denotes the Haldane gap and v is the velocity of the quasi particle. They described the asymptotic effects of boundary scattering and intermagnon interactions in terms of the scattering lengths, a_b and a , which appear in k_{eff} . When boundary tuning is applied by introducing an antiferromagnetic coupling J_{end} between the $S = 1$ spin chain and the extra real $S = 1/2$ spin, these scattering lengths might be effected. This idea motivated us to study low-lying elementary exci-

tations using both the DMRG and NLSM methods by describing the bulk properties and the boundary scattering effects in terms of an effective theory. In this work, using the DMRG method, the energy dispersion of various magnon modes was determined for $S = 1$ Heisenberg systems with up to 2048 spins. Finite-size scaling analysis was performed to determine the boundary scattering length and the inter-magnon scattering length, in addition to Δ and v in the thermodynamic limit. We used a relation of the correlation length $\xi \sim v/\Delta$, which is known to hold approximately in the integer-spin AF Heisenberg chain.^{48,49} We found that a_b changed sign around a critical value of J_{end} . This value should be identical to that required to make local quantities such as the local bond energy of the ground state and the spin density of long-wavelength magnons uniform.^{36,39,50,51} In addition, a divergence-like behavior of a_b was detected around this critical value denoted as J_{end}^c . However, the inter-magnon scattering length was found to be constant at $a = -0.383(6)\xi$ irrespective of J_{end} . In this derivation, Δ , v , and ξ were confirmed to be always independent of J_{end} in the thermodynamic limit. This allows the low-lying elementary excitations to be effectively described. The results indicated the presence of both itinerating magnons (IMs) and boundary magnons (BMs) bound at the ends. At J_{end}^c , the diagonal magnetization induced by an IM shows a flat structure around the center of the system when $L \gg \xi$, with L being the number of $S = 1$ spins. Both the diverging behavior of a_b and the uniform distribution of the long-wavelength magnons confirm the realization of bulk characteristics in an elementary excitation at the critical point J_{end}^c , where the ground state also has a uniform nature around the center of the system.

Furthermore, this work clearly resolves the problem pointed out by Todo and Kato³⁷; there is disagreement between the DMRG⁵² and quantum Monte Carlo (QMC) simulation results³⁷ with respect to estimation of the excitation gap in the $S = 2$ AF Heisenberg model. The reason for this disagreement might be an inappropriate scaling assumption in the DMRG study. This work applies finite-size scaling analysis to the excitation gap in

the $S = 2$ AF chain, and shows for the first time that the corrected gap is within the error bar of the QMC value.

II. EFFECTIVE HAMILTONIAN

We consider a $S = 1$ AF chain with boundary $S = 1/2$ spins \mathbf{s}_j with $j = 0$ or $L + 1$, which is described by the following Hamiltonian.

$$H(J_{\text{end}}) = \sum_{i=1}^{L-1} \mathbf{S}_i \cdot \mathbf{S}_{i+1} + J_{\text{end}}(\mathbf{s}_0 \cdot \mathbf{S}_1 + \mathbf{S}_L \cdot \mathbf{s}_{L+1}), \quad (1)$$

where \mathbf{S}_i represents the $S = 1$ operator at the i -th site.

The low-energy physics of the Hamiltonian in Eq. (1) can be understood by using an approximate mapping onto the NLSM.^{34,35,41,42} We let $L \rightarrow \infty$, keeping $X = Lb$ constant, with b being the lattice spacing. Taking into account the effective $S = 1/2$ boundary modes $\mathbf{s}_j^{\text{eff}}$, we obtain the following expression,

$$\begin{aligned} H_{\text{eff}} = & H_{\text{NLSM}} + \lambda_s [\phi(0) \cdot \mathbf{s}_1^{\text{eff}} + (-1)^L \phi(X) \cdot \mathbf{s}_L^{\text{eff}}] \\ & + \lambda_u [\mathbf{l}(0) \cdot \mathbf{s}_1^{\text{eff}} + \mathbf{l}(X) \cdot \mathbf{s}_L^{\text{eff}}] \\ & + \lambda'_s [\phi(0) \cdot \mathbf{s}_0 + (-1)^L \phi(X) \cdot \mathbf{s}_{L+1}] \\ & + \lambda'_u [\mathbf{l}(0) \cdot \mathbf{s}_0 + \mathbf{l}(X) \cdot \mathbf{s}_{L+1}] \\ & + J_{\text{end}}^{\text{eff}} [\mathbf{s}_1^{\text{eff}} \cdot \mathbf{s}_0 + \mathbf{s}_L^{\text{eff}} \cdot \mathbf{s}_{L+1}], \end{aligned} \quad (2)$$

with the bulk part of the NLSM expressed as

$$H_{\text{NLSM}} = \frac{v}{2} \int_0^X dx \left[g\mathbf{l}^2 + \frac{1}{g} \left(\frac{\partial \phi}{\partial x} \right)^2 \right], \quad (3)$$

where ϕ and $\mathbf{l} \equiv (1/vg)\phi \times \partial_t \phi$ are low-energy Fourier modes of the spin operators with wave vectors near π and 0. The coupling parameter and the velocity are given as $g = \frac{2}{S}$, $v = 2S$. Since all the bare couplings are antiferromagnetic, solutions for the bulk fields follow the Neumann boundary conditions (NBC) : $d\phi/dx|_{x=0,X} = 0$.⁴⁷ The λ_u and λ'_u terms produce an effective boundary repulsive potential on an IM, and $J_{\text{end}}^{\text{eff}}$ is a renormalized coupling constant.

The validity of this description is also confirmed by examining the spin density of an IM shown in Fig. 1. When J_{end} is larger than J_{end}^c , the lowest triplet mode has itinerating behavior. Indeed, we see that $\langle S_i^z \rangle$ exhibits a cosine-like behavior for $J_{\text{end}} = 1.0$ owing to both strong repulsive coupling via λ_u and λ'_u , and the NBC on $\phi(x)$. When J_{end} approaches $J_{\text{end}}^c \sim 0.51$, the IM mode becomes uniform around the center of the chain but $\langle S_i^z \rangle$ exhibits damped oscillations near the two ends. This known solution suggests that the mode should continuously change into an end mode $\mathbf{s}_j^{\text{eff}}$ in the low-energy eigenstate when $J_{\text{eff}} < J_{\text{end}}^c$.

Thus, the dispersion relation for N itinerating magnon modes at low energies in the dilute limit may be simply reproduced by a nonrelativistic effective Hamiltonian for

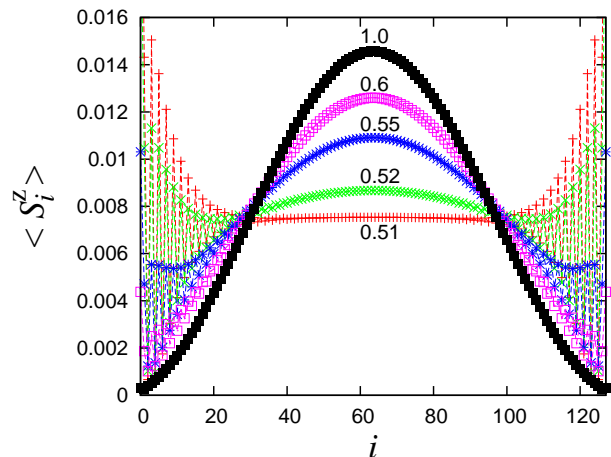


FIG. 1. (Color online) Distribution of local magnetization $\langle S_j^z \rangle$ for a single magnon state with $S_{\text{tot}} = 1$ for various values of J_{end} .

N virtual particles,

$$\begin{aligned} H_{\text{eff}}(J_{\text{end}}) = & \frac{1}{2m} \sum_{i=1}^N \frac{d^2}{dx_i^2} + \sum_{\langle i,j \rangle} V(x_i - x_j) \\ & + \sum_{i=1}^N [V_b(J_{\text{end}}, x_i) + V_b(J_{\text{end}}, X - x_i)], \end{aligned} \quad (4)$$

where $0 \leq x_j \leq X$, with a wavefunction obeying the Neumann boundary condition: $\partial_j \psi(x_1, \dots, x_N)|_{x_j=0,X} = 0$. Here we use the Einstein relation $m \equiv \Delta/v^2$. Effective short-range interactions between IMs and between an IM and a BM are represented by V and V_b , respectively. We expect they are short-range function with range of the order of the correlation length ξ . All of the effects of J_{end} are produced by the boundary potential $V_b(J_{\text{end}}, x)$. In the asymptotic region, the effects of V and V_b appear as scattering phase shifts, which are represented by a and a_b .

We now identify low-lying magnon modes. Each mode is specified by a total spin of S_{tot} . When J_{end} is small and positive, since we have two effective $S = 1/2$ spins creating the bulk low-lying triplet and two real $S = 1/2$ spins, we need to polarize these four spins before we can create one IM. In this case, the effective chain length for the IM becomes $L - 2a_b$ and $k_{\text{eff}} = \pi/(L - 2a_b)$, when the system is about two times longer than the correlation length ξ . Therefore, we have the relation:

$$E_{32} = \sqrt{\Delta^2 + v^2 \sin^2 \frac{\pi}{L - 2a_b}}, \quad (5)$$

where $E_{ji} = E_j - E_i$ and E_j and E_i are the lowest energy of the $S_{\text{tot}} = j$ and $S_{\text{tot}} = i$ states. The energy spectrum E_{42} for two IMs is given by

$$E_{42} = \sum_{j=1}^2 \sqrt{\Delta^2 + v^2 \sin^2 \frac{j\pi}{L - 2a_b - a}}, \quad (6)$$

where we use the small- k approximation for the magnon-magnon phase shift. When J_{end} becomes large enough, the effective boundary $S = 1/2$ modes couple strongly with the real $S = 1/2$ spins. In this condition, the low-lying magnon states are IMs, and the formulas for E_{10} and E_{20} are, respectively, similar to Eq. (5) and Eq. (6). Thus, we can conclude that a crossover value of J_{end}^c exists, where the low energy spectrum changes qualitatively.

III. NUMERICAL RESULTS

We used the non-Abelian DMRG method (NA-DMRG)⁵³ to estimate the energy spectrum of the lowest $S_{\text{tot}} = 0, 1, 2, 3$, and 4 states for finite systems. Numerical convergence during finite system sweeping was accelerated by the use of a wave function prediction method.^{54–59} Since the number of kept states for the block spin is up to $m_s = 512$, the truncation error is smaller than 1.0×10^{12} in the lowest $S_{\text{tot}} = 4$ state. This corresponds to a number of kept states of $m_{sz} \sim 2500 - 2700$ in the standard DMRG. In this case, the numerical cost of the standard DMRG is about 110 - 140 times higher than that of NA-DMRG, because in the DMRG it varies as the cube of the number of kept states. The system size $L + 2$ is up to 2048, where the two extra spins indicate the boundary $S = 1/2$ spins.

The energy of a single IM as a function of the system size is shown in Fig. 2. The target energy spectrum is E_{32} when $J_{\text{end}} = 0$, and E_{10} when $J_{\text{end}} = 0.6$ or 1. To estimate Δ , v and a_b , we generated sequences $A^*(L_0 + 2)$ for different values of $L = L_0$, where $A^*(L)$ denotes finite values of $A = \Delta, v$ and a_b in the thermodynamic limit. The sequences were determined by least square fitting with the function $\sqrt{\Delta^2 + v^2 \sin^2 \frac{\pi}{L - 2a_b}}$ for IM energies of $L + 2 = 2^\ell(L_0 + 2)$, where $\ell = 0, \pm 1$. The value of A was estimated by power-law extrapolation with elements of $A^*(512)$ and $A^*(1024)$. The estimation error was taken to be $|A - A^*(1024)|$. Based on the optimum boundary scattering length $a_b(J_{\text{end}})$ for each J_{end} , we found a universal finite size dependence for a fixed energy gap Δ and spin velocity v . As a result, we showed that only the boundary scattering length a_b was affected by changing J_{end} , whereas Δ and v were independent of J_{end} (See Table I). This result is consistent with the effective model in Eq. (4).

The estimated values of Δ , v , and $\xi = v/\Delta$ are consistent to within $\Delta = 0.4104792485(4)$, $v = 2.46685(2)$ and $\xi = 6.00967(5)$, respectively, except for a somewhat larger error at $J_{\text{end}} = 0.4$ and 0.6, which are closest to J_{end}^c . Since our data is obtained by extrapolation using system sizes larger than those treated in former studies,^{36,37} our results show meaningful differences. The reported value of $a_b(J_{\text{end}} = 0) = -1$ in Ref. [47] is about three times larger than our result of $a_b(J_{\text{end}} = 0) = -0.3748(1)$. The value of $a_b(J_{\text{end}})$

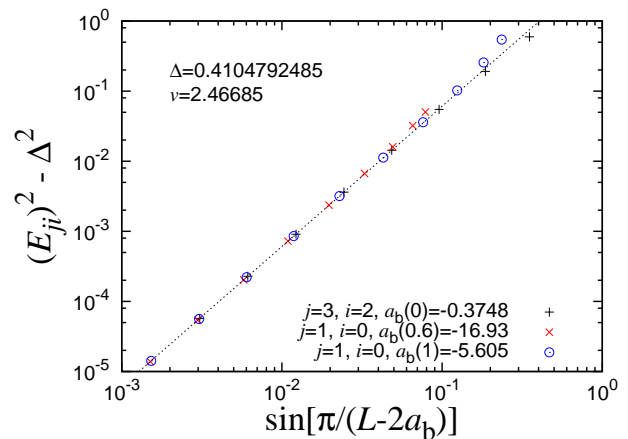


FIG. 2. (Color online) Single magnon energy with J_{end} under the condition $m_s = 512$ ($m_{sz} \sim 2500$). The dotted line represents $v^2 \sin^2(\pi/(L - 2a_b))$.

changes rather dramatically with J_{end} , (Fig. 3) with a change in sign even occurring around $J_{\text{end}} \sim 0.5$. The values seem to diverge around J_{end}^c . When the boundary scattering length becomes $a_b \rightarrow -\infty$, $k_{\text{eff}} = \pi/(L - 2a_b)$ approaches zero, and the energy of the lowest IM is almost at its minimum value, Δ , and is independent of J_{end} . This is consistent with the report in Ref. [36,50]. However, we should note that the above picture holds only when $L \gg a_b$, requiring a high performance simulation tool such as NA-DMRG.

In the same manner, using the estimated Δ , v , and a_b , we determined the inter-magnon scattering length a . The target energy spectrum is E_{42} when $J_{\text{end}} < J_{\text{end}}^c$, and is E_{20} when $J_{\text{end}} > J_{\text{end}}^c$. With a common a , universal behavior is observed in the large L region. The estimated values of a are consistent to within $a = -2.30(4) = -0.383(6)\xi$ except for a somewhat larger error at $J_{\text{end}} = 0.4$ and 0.6. (See Table I and Fig. 3.) Thus, we conclude that the value of a is independent of J_{end} . The estimated value of a is comparable to $a = -0.32\xi$ in Ref. [47]. In Fig. 3, the dotted line represents $J_{\text{end}} = 0.50865$ determined in Ref. [39].

IV. APPLICATION TO $S = 2$ HEISENBERG CHAIN AND CONCLUSIONS

We have shown that the energy spectrum modified by the tuning parameter J_{end} can be fitted using an effective massive relativistic dispersion with a boundary scattering length $a_b(J_{\text{end}})$ modified for lattice models. The intermagnon scattering length a is constant irrespective of J_{end} , as well as other bulk quantities including the Haldane gap, the magnon velocity, and the correlation length. In contrast, $a_b(J_{\text{end}})$ drastically changes around $J_{\text{end}} \sim 0.5$, representing a crossover point for the physics at the boundary.

TABLE I. Results of numerical simulations for a single itinerating magnon, showing magnon energy Δ , magnon velocity v , boundary scattering length a_b , intermagnon scattering length a , and correlation length $\xi = v/\Delta$, a_b/ξ and a/ξ .

J_{end}	Δ	v	a_b	a	ξ	a_b/ξ	a/ξ
0	0.4104792487(1)	2.466838(1)	-0.3748(1)	-2.30(2)	6.009654(1)	-0.06237(2)	-0.383(4)
0.1	0.4104792486(1)	2.466844(2)	-0.0836(3)	-2.301(2)	6.009669(4)	-0.01391(5)	-0.3830(4)
0.2	0.4104792487(1)	2.46684(1)	0.540(2)	-2.303(5)	6.00966(3)	0.0898(3)	-0.3833(9)
0.3	0.4104792486(4)	2.46684(4)	2.081(8)	-2.30(4)	6.0096(1)	0.346(1)	-0.384(6)
0.4	0.410479248(2)	2.4668(3)	7.33(5)	-2.3(2)	6.0098(7)	1.220(9)	-0.38(5)
0.6	0.410479248(2)	2.4668(2)	-16.93(2)	-2.3(2)	6.0096(5)	-2.821(6)	-0.38(3)
0.7	0.4104792483(2)	2.46685(3)	-9.586(5)	-2.30(3)	6.00968(7)	-1.5951(9)	-0.382(4)
0.8	0.4104792483(2)	2.46685(2)	-7.317(3)	-2.30(2)	6.00968(4)	-1.2176(5)	-0.383(3)
0.9	0.4104792483(2)	2.46685(2)	-6.233(3)	-2.30(2)	6.00968(4)	-1.0372(5)	-0.383(3)
1.0	0.4104792485(1)	2.46684(1)	-5.605(3)	-2.30(2)	6.00967(4)	-0.9328(5)	-0.383(3)

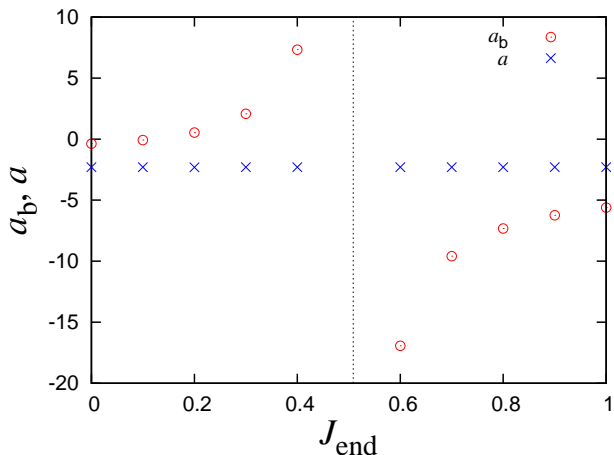


FIG. 3. (Color online) Boundary scattering length and intermagnon scattering length as a function of J_{end} . The dotted line represents $J_{\text{end}} = 0.50865$.

Analysis of the boundary scattering length and intermagnon scattering length was also carried out for a $S = 2$ AF Heisenberg chain, where \mathbf{S}_i and \mathbf{s}_i in the Hamiltonian in eq. (1) represent the $S = 2$ and $S = 1$ operators, respectively. In addition, we choose $J_{\text{end}} = 1$, so that the low-lying magnon states are IMs, and a similar formula for E_{10} is obtained to that shown in Eq. (5). Our data was taken using $m_s = 1024$, which corresponds to $m_{sz} \sim 6000$, and large systems up to $L + 2 = 2048$. The truncation error is smaller than 1×10^{-11} . Note that the numerical cost using NA-DMRG is about 200 times less than that for the standard DMRG in this case. In contrast to a former report,⁶⁰ our results suggests a large value of $a_b(J_{\text{end}} = 1) = -33(1) = -0.67(2)\xi$. Our calculations give the excitation gap $\Delta = 0.0891623(9)$, the spin velocity $v = 4.42(1)$, and the correlation length $\xi = 49.6(1)$. In particular, the value of Δ obtained in the present study is consistent with the value of 0.08917(4)

determined by quantum Monte Carlo simulations.³⁷ The estimate of the Haldane gap has thus been improved by two more significant digits. This indicates the ability of the effective theory to correctly describe the low-energy physics, and the usefulness of the proposed numerical approach is studying such problems

It would be of interest to apply the approach used in this work to finite size scaling with different boundary tuning methods such as hyperbolic deformation.^{46,61,62} In such a situation, the excited quasi particle is weakly confined near the center of the system under the deformation. In Ref. [61], we showed that it is necessary to introduce an additional parameter d and replace $L + 1$ by $L + d$ in order to reduce higher-order corrections. This replacement is introduced in the effective model shown in Eq. (4) by considering the effective boundary scattering. The boundary scattering length has an important and universal influence on excitation energy scaling as long as there are chain ends.

In this work, a relation $\xi = v/\Delta$ is used to estimate the correlation length in each spin- S chain. If we use an assumption for a relation between the low-energy dispersion curve and the ground state correlation length, namely $\sinh \xi^{-1} = \Delta/v$ in this case,⁶³ the correlation lengths are evaluated as 6.03720(9) in $S = 1$ and 49.6(1) in $S = 2$. In the case of $S = 1$, we have a meaningful different value from the former estimation. On the contrary, the difference is not confirmed in the case of $S = 2$. To find correct relation between the low-energy dispersion and the correlation length in each spin- S AF Heisenberg chain is a future issue.

For a final development of the low-lying effective field theory to describe the low-lying magnon dispersions, discussions for rigorous results of wave functions and energy dispersions for low-lying states are important. The effective dispersion relation of $\sqrt{\Delta^2 + v^2 \sin^2 k_{\text{eff}}}$ is known to appear in the Haldane phase⁶⁴ and also in the massive phase of the $S = 1/2$ XXZ model.⁶⁵ The Bethe-ansatz solutions for OBC suggest that an analogous crossover

from an IM with real k_{eff} to a BM with a damping nature can be found as a continuous change from a real to an imaginary rapidity.⁶⁶

ACKNOWLEDGMENTS

This work was supported in part by a Grant-in-Aid for JSPS Fellows, Grant-in-Aids (No. 19051016), Global COE Program (Core Research and Engineering of Advanced Materials - Interdisciplinary Education Center for Materials Science) from the Ministry of Education, Culture, Sports, Science and Technology of Japan.

-
- * ueda@aquarius.mp.es.osaka-u.ac.jp
 † kabe@mp.es.osaka-u.ac.jp
- ³⁴ F. D. M. Haldane, Phys. Lett. A **93**, 464 (1983).
³⁵ F. D. M. Haldane, Phys. Rev. Lett. **50**, 1153 (1983).
³⁶ S. R. White and D. A. Huse, Phys. Rev. B **48**, 3844 (1993).
³⁷ S. Todo and K. Kato, Phys. Rev. Lett. **87**, 047203 (2001).
³⁸ H. Nakano and A. Terai, J. Phys. Soc. Jpn. **78**, 014003 (2009).
³⁹ S. R. White and I. Affleck, Phys. Rev. B **77**, 134437 (2008).
⁴⁰ J. Haegeman, B. Pirvu, D. J. Weir, J. I. Cirac, T. J. Osborne, H. Verschelde, and F. Verstraete, arXiv:1103.2286v1 [quant-ph].
⁴¹ I. Afflek, Nucl. Phys. **B257**, 397 (1985).
⁴² I. Affleck, J. Phys.: Condens. Matter **1**, 3047 (1989).
⁴³ T. Kennedy and H. Tasaki, Phys. Rev. B **45**, 304 (1992).
⁴⁴ S. R. White, Phys. Rev. Lett. **69**, 2863 (1992).
⁴⁵ S. R. White, Phys. Rev. B **48**, 10345 (1993).
⁴⁶ H. Ueda and T. Nishino, J. Phys. Soc. Jpn. **78**, 014001 (2009).
⁴⁷ J. Lou, S. Qin, T.-K. Ng, Z. Su, and I. Affleck, Phys. Rev. B **62**, 3786 (2000).
⁴⁸ E. S. Sørensen and I. Affleck, Phys. Rev. Lett. **71**, 1633 (1993).
⁴⁹ S. Qin, X. Wang, and L. Yu, Phys. Rev. B **56**, R14251 (1997).
⁵⁰ U. Schollwöck, O. Golinelli, and T. Jolicœur, Phys. Rev. B **54**, 4038 (1996).
⁵¹ H. Ueda, H. Nakano, K. Kusakabe, and T. Nishino, (), arXiv:0812.4513v2 [cond-mat.stat-mech].
⁵² X. Wang, S. Qin, and L. Yu, Phys. Rev. B **60**, 14529 (1999).
⁵³ I. P. McCulloch and M. Gulácsi, Europhys. Lett. **57**, 852 (2002).
⁵⁴ S. R. White, Phys. Rev. Lett. **77**, 3633 (1996).
⁵⁵ T. Nishino and K. Okunishi, J. Phys. Soc. Jpn. **64**, 4084 (1995).
⁵⁶ K. Ueda, T. Nishino, K. Okunishi, Y. Hieida, R. Derian, and A. Gendiar, J. Phys. Soc. Jan **75**, 014003 (2006).
⁵⁷ H. Ueda, T. Nishino, and K. Kusakabe, J. Phys. Soc. Jan **77**, 114002 (2008).
⁵⁸ I. P. McCulloch, arXiv:0804.2509v1 [cond-mat.str-el].
⁵⁹ H. Ueda, A. Gendiar, and T. Nishino, J. Phys. Soc. Jan **79**, 044001 (2010).
⁶⁰ J. Lou, S. Qin, and Z. Su, Phys. Rev. B **62**, 13832 (2000).
⁶¹ H. Ueda, H. Nakano, K. Kusakabe, and T. Nishino, Prog. Theor. Phys. **124**, 389 (2010).
⁶² H. Ueda, H. Nakano, K. Kusakabe, and T. Nishino, (), arXiv:1102.0845v1 [cond-mat.str-el].
⁶³ K. Okunishi, Y. Akutsu, N. Akutsu, and T. Yamamoto, Phys. Rev. B **64**, 104432 (2001).
⁶⁴ S. Ma, C. Broholm, D. H. Reich, B. J. Sternlieb, and R. W. Erwin, Phys. Rev. Lett. **69**, 3571 (1992).
⁶⁵ M. Takahashi, *Thermodynamics of One-Dimensional Solvable Models* (Cambridge-Univ-Press, Cambridge, 1999).
⁶⁶ T. Deguchi, R. Yue, and K. Kusakabe, J. Phys. A: Math. Gen. **31**, 7315 (1998).
³⁴ F. D. M. Haldane, Phys. Lett. A **93**, 464 (1983).
³⁵ F. D. M. Haldane, Phys. Rev. Lett. **50**, 1153 (1983).
³⁶ S. R. White and D. A. Huse, Phys. Rev. B **48**, 3844 (1993).
³⁷ S. Todo and K. Kato, Phys. Rev. Lett. **87**, 047203 (2001).
³⁸ H. Nakano and A. Terai, J. Phys. Soc. Jpn. **78**, 014003 (2009).
³⁹ S. R. White and I. Affleck, Phys. Rev. B **77**, 134437 (2008).
⁴⁰ J. Haegeman, B. Pirvu, D. J. Weir, J. I. Cirac, T. J. Osborne, H. Verschelde, and F. Verstraete, arXiv:1103.2286v1 [quant-ph].
⁴¹ I. Afflek, Nucl. Phys. **B257**, 397 (1985).
⁴² I. Affleck, J. Phys.: Condens. Matter **1**, 3047 (1989).
⁴³ T. Kennedy and H. Tasaki, Phys. Rev. B **45**, 304 (1992).
⁴⁴ S. R. White, Phys. Rev. Lett. **69**, 2863 (1992).
⁴⁵ S. R. White, Phys. Rev. B **48**, 10345 (1993).
⁴⁶ H. Ueda and T. Nishino, J. Phys. Soc. Jpn. **78**, 014001 (2009).
⁴⁷ J. Lou, S. Qin, T.-K. Ng, Z. Su, and I. Affleck, Phys. Rev. B **62**, 3786 (2000).
⁴⁸ E. S. Sørensen and I. Affleck, Phys. Rev. Lett. **71**, 1633 (1993).
⁴⁹ S. Qin, X. Wang, and L. Yu, Phys. Rev. B **56**, R14251 (1997).
⁵⁰ U. Schollwöck, O. Golinelli, and T. Jolicœur, Phys. Rev. B **54**, 4038 (1996).
⁵¹ H. Ueda, H. Nakano, K. Kusakabe, and T. Nishino, (), arXiv:0812.4513v2 [cond-mat.stat-mech].
⁵² X. Wang, S. Qin, and L. Yu, Phys. Rev. B **60**, 14529 (1999).
⁵³ I. P. McCulloch and M. Gulácsi, Europhys. Lett. **57**, 852 (2002).
⁵⁴ S. R. White, Phys. Rev. Lett. **77**, 3633 (1996).
⁵⁵ T. Nishino and K. Okunishi, J. Phys. Soc. Jpn. **64**, 4084 (1995).
⁵⁶ K. Ueda, T. Nishino, K. Okunishi, Y. Hieida, R. Derian, and A. Gendiar, J. Phys. Soc. Jan **75**, 014003 (2006).
⁵⁷ H. Ueda, T. Nishino, and K. Kusakabe, J. Phys. Soc. Jan **77**, 114002 (2008).
⁵⁸ I. P. McCulloch, arXiv:0804.2509v1 [cond-mat.str-el].
⁵⁹ H. Ueda, A. Gendiar, and T. Nishino, J. Phys. Soc. Jan **79**, 044001 (2010).
⁶⁰ J. Lou, S. Qin, and Z. Su, Phys. Rev. B **62**, 13832 (2000).

- ⁶¹ H. Ueda, H. Nakano, K. Kusakabe, and T. Nishino, *Prog. Theor. Phys.* **124**, 389 (2010).
- ⁶² H. Ueda, H. Nakano, K. Kusakabe, and T. Nishino, (), [arXiv:1102.0845v1](https://arxiv.org/abs/1102.0845v1) [cond-mat.str-el].
- ⁶³ K. Okunishi, Y. Akutsu, N. Akutsu, and T. Yamamoto, *Phys. Rev. B* **64**, 104432 (2001).
- ⁶⁴ S. Ma, C. Broholm, D. H. Reich, B. J. Sternlieb, and R. W. Erwin, *Phys. Rev. Lett.* **69**, 3571 (1992).
- ⁶⁵ M. Takahashi, *Thermodynamics of One-Dimensional Solvable Models* (Cambridge-Univ-Press, Cambridge, 1999).
- ⁶⁶ T. Deguchi, R. Yue, and K. Kusakabe, *J. Phys. A: Math. Gen.* **31**, 7315 (1998).